

Enhanced Efficacy of Therapeutic Cancer Vaccines Produced by Co-Treatment with *Mycobacterium tuberculosis* Heparin-Binding Hemagglutinin, a Novel TLR4 Agonist

In Duk Jung¹, Soo Kyung Jeong¹, Chang-Min Lee¹, Kyung Tae Noh¹, Deok Rim Heo¹, Yong Kyoo Shin², Cheol-Heui Yun³, Won-Jung Koh⁴, Shizuo Akira⁵, Jake Whang⁶, Hwa-Jung Kim⁶, Won Sun Park⁷, Sung Jae Shin⁶, and Yeong-Min Park¹

Abstract

Effective activation of dendritic cells (DCs) toward T helper (Th)-1 cell polarization would improve DC-based antitumor immunotherapy, helping promote the development of immunotherapeutic vaccines based on T-cell immunity. To achieve this goal, it is essential to develop effective immune adjuvants that can induce powerful Th1 cell immune responses. The pathogenic organism *Mycobacterium tuberculosis* includes certain constituents, such as heparin-binding hemagglutinin (HBHA), that possess a strong immunostimulatory potential. In this study, we report the first clarification of the functions and precise mechanism of HBHA in immune stimulation settings relevant to cancer. HBHA induced DC maturation in a TLR4-dependent manner, elevating expression of the surface molecules CD40, CD80, and CD86, MHC classes I and II and the proinflammatory cytokines IL-6, IL-12, IL-1 β , TNF- α , and CCR7, as well as stimulating the migratory capacity of DCs *in vitro* and *in vivo*. Mechanistic investigations established that MyD88 and TRIF signaling pathways downstream of TLR4 mediated secretion of HBHA-induced proinflammatory cytokines. HBHA-treated DCs activated naïve T cells, polarized CD4⁺ and CD8⁺ T cells to secrete IFN- γ , and induced T-cell-mediated cytotoxicity. Notably, systemic administration of DCs that were HBHA-treated and OVA₂₅₁₋₂₆₄-pulsed *ex vivo* greatly strengthened immune priming *in vivo*, inducing a dramatic regression of tumor growth associated with long-term survival in a murine E.G7 thymoma model. Together, our findings highlight HBHA as an immune adjuvant that favors Th1 polarization and DC function for potential applications in DC-based antitumor immunotherapy. *Cancer Res*; 71(8); 2858–70. ©2011 AACR.

Authors' Affiliations: ¹Department of Microbiology and Immunology, School of Medicine, Pusan National University, Beom-eo Ri, Mulgum Eop, Yangsan, Gyeongsangnam-do, Republic of Korea; ²Department of Pharmacology, College of Medicine, Chung-Ang University, Dongjak-Ku, Seoul, Republic of Korea; ³Department of Agricultural Biotechnology and Research Institute for Agriculture and Life Sciences, Seoul National University, Gwanak-gu, Seoul, Republic of Korea; ⁴Division of Pulmonary and Critical Care Medicine, Department of Medicine, Samsung Medical Center, Sungkyunkwan University School of Medicine, Gangnam-gu, Seoul, Republic of Korea; ⁵Laboratory of Host Defense, WPI Immunology Frontier Research Center, Osaka University, Osaka, Japan; ⁶Department of Microbiology, College of Medicine, Chungnam National University, Munwha-Dong, Jung-Ku, Daejeon, Republic of Korea; and ⁷Department of Physiology, Kangwon National University, School of Medicine, Chuncheon, Republic of Korea

Note: Supplementary data for this article are available at Cancer Research Online (<http://cancerres.aacrjournals.org/>).

S. J. Shin and Y.-M. Park contributed equally as a corresponding author.

Corresponding Author: Yeong-Min Park, Department of Microbiology and Immunology, School of Medicine, Pusan National University, Beom-eo Ri, Mulgum Eop, Yangsan, Gyeongsangnam-do 626-770, South Korea. Phone: +82-51-510-8097; Fax: +82-55-382-8090; E-mail: immunpym@pusan.ac.kr.

doi: 10.1158/0008-5472.CAN-10-3487

©2011 American Association for Cancer Research.

Introduction

Owing to the immunosuppressive environment within a tumor, effective antitumor therapy requires the powerful induction of appropriate immune responses. Dendritic cell (DC)-based antitumor immunotherapy is mediated by specialized interactions between DCs and T lymphocytes (1).

For all DC-based antitumor immunotherapeutic strategies, several factors that relate to the *in vitro* manipulation of DCs are important for the induction of a powerful immune response in patients. These factors include DC lineage, amount and type of antigen (Ag) loading on DCs, maturation stage of DCs, and route of injection (2). Evidence has suggested that immunostimulatory adjuvants are critical for the maturation of immature DCs, which boosts the activity of DCs as well as enhances T-cell-mediated immune responses. Therefore, the use of poorly immunogenic Ags combined with effective adjuvants can enhance specific T helper (Th)-1 cell responses. Although many adjuvants have been discovered, the use of adjuvant(s) for DC-based antitumor immunotherapy is limited due to safety concerns and unforeseen inappropriate immune responses (3).

Because Toll-like receptor (TLR) activation usually induces Th1 responses, TLR ligands are potential candidates for immunostimulatory adjuvants in anticancer therapy (4). On recognition of their ligands, TLRs mediate signals via 2 intracytoplasmic adaptor molecules, myeloid differentiation primary response protein (MyD88) and Toll/IL-1R domain-containing adaptor inducing IFN β (TRIF), which are used by all TLRs except TLR3 (5). In the recent years, synthetic agonists of TLR3, TLR4, TLR5, TLR7, TLR8, and TLR9 have been identified as suitable immunostimulants (6–11). In fact, based on the efficacy of TLR agonists, the use of TLR ligands as adjuvants in humans is likely to increase in the near future. Furthermore, DC activation by various microbial components through TLRs' signaling is a critical link between innate and adaptive immunity and is crucial for the generation of protective immune responses.

Adjuvants inducing Th1-type responses are essential for effective immunotherapeutic strategies. Because some components expressed by organism of the genus *Mycobacterium* and related genera, showed strong Th1-type adjuvancy, a significant effort has been focused on identifying and characterizing these mycobacterial proteins (12). Although an immunotherapeutic approach using mycobacterial Ags appears to be clinically effective, the precise mechanism by which these Ags mediate immune stimulation has not been adequately clarified (12).

To date, it is known that *M. tuberculosis* interacts with Ag-presenting cells, specifically DCs (13). In addition, we recently showed that the *Mycobacterium avium* protein fibronectin attachment protein induces DC maturation and Th1 polarization (14). These reports provide direct evidences for the potential use of mycobacterial proteins in DC-based antitumor immunotherapies to induce the activation of T-cell-mediated cytotoxicity.

The *M. tuberculosis* protein, heparin-binding hemagglutinin (HBHA) was recently identified as surface-exposed and secreted Ag. This protein is a virulence factor that promotes bacterial aggregation, adhesion to heparin sulfate proteoglycans of nonphagocytic cells, and dissemination of tubercle bacilli from the lungs to other tissues in patients with tuberculosis (15, 16). HBHA induces protective immunity against *M. tuberculosis* by triggering the interferon (IFN)- γ production in CD4⁺ and CD8⁺ T lymphocytes (17). Thus, it could serve as an immunoadjuvants to design and develop immunotherapies against various diseases including if the detailed elucidation of the cellular immune responses to HBHA. However, very little is known about the antitumor activity of HBHA mediated by inducing DC maturation and, hence, promoting T-cell immunity.

To clarify the action mechanism of HBHA and its potential use as an adjuvant in DC-based antitumor immunotherapies, we investigated whether HBHA exhibits an antitumor effect in DC-based vaccination in a mouse model.

Materials and Methods

Mice

Male 6–8-week old C57BL/6 (H-2K^b and I-A^b) mice were purchased from the Korean Institute of Chemistry Technology

(Daejeon, Korea). C57BL/6 OT-1 T-cell receptor (TCR) transgenic mice, C57BL/6J TLR2 knockout mice (*TLR2*^{-/-}; B6.129-Tlr2^{tm1Kir/J}), and C57BL/10 TLR4 knockout mice (*TLR4*^{-/-}; C57BL/10ScNJ) were purchased at 6–8 weeks of age from the Jackson Laboratory (Bar Harbor, ME). The TLR9-knockout mice, originally from Dr. Shizuo Akira (Osaka, Japan), were obtained from Dr. Seong-Kug Eo (Chonbuk National University, Korea). All mice were housed in a specific pathogen-free environment and used in accordance with the institutional guidelines for animal care.

Cell lines

The cell lines EL4, a thymoma-derived cell line from the C57BL/6 (H-2K^b and I-A^b) mouse, and E.G7, an ovalbumin (OVA)-expressing EL4 variant, were purchased from ATCC and cultured in RPMI 1640 supplemented with 10% heat-inactivated FBS, 100 U/mL penicillin, 100 μ g/mL streptomycin, and 10 mmol/L L-glutamine (all purchased from Invitrogen) at 37°C with 5% CO₂.

Reagents and antibodies

Recombinant mouse granulocyte-macrophage colony-stimulating factor (GM-CSF), interleukin (rmIL)-4, chemokine ligand (CCL) 19, and the fluorescein isothiocyanate (FITC)-annexin V/propidium iodine kit were purchased from R&D Systems. Dextran-FITC (40,000 Da) was purchased from Sigma-Aldrich. Lipopolysaccharide (LPS, from *Escherichia coli* O111:B4) was purchased from Invivogen. Peptron synthesized the OT-I peptide (OVA_{257–264}) and OT-II peptide (OVA_{323–339}). The following FITC- or phycoerythrin (PE)-conjugated monoclonal antibodies (Abs) were purchased from BD Biosciences: CD11c (HL3), CD40 (HM40-3), CD80 (16-10A1), CD86 (GL1), Iab β -chain (AF-120.1), H-2K^b (AF6-88.5), CCR7 (CD197), IL-10 (JESS-16E3), and IL-12p40/p70 (C15.6). Alexa568 and Alexa488 conjugated anti-mouse IgG Abs as secondary Abs were purchased from Invitrogen. FITC-conjugated mouse IgG Abs and cytokine ELISA kits for murine IL-1 β , IL-2, IL-6, IL-10, IL-12p70, tumor necrosis factor (TNF)- α , and IFN- γ were purchased from eBiosciences.

Expression and purification of recombinant HBHA

Dr. G. Delogu (University of Sassari, Sassari, Italy) kindly provided the pMV3-38 plasmid (pMV206-based construct) containing the full-length HBHA open reading frame. Methylated-recombinant HBHA expressed in *Mycobacterium smegmatis* was purified as previously described (18). Preparation of *M. smegmatis* competent cells and electroporation procedures were performed as previously described (19). A Detoxi-Gel™ Endotoxin Removing Gel (Pierce) was used to remove endotoxin. Finally, the protein concentration was determined using a BCA Protein Assay Kit (Pierce) and the purified protein was stored at -80°C in aliquots until use in the subsequent experiments. To evaluate the purity of rHBHA, SDS-PAGE followed by Coomassie blue (CB) staining, immunoblot assay using antihistidine antibody and silver nitrate staining as previously described (PMID: 17487168).

Generation and culture of DCs

Bone marrow-derived DCs were isolated and cultured as recently described (20). In certain experiments, DCs were labeled with bead-conjugated anti-CD11c mAb and positively selected (>90%) according to the manufacturer's instructions (LS columns; Miltenyi Biotec).

Therapeutic implanted tumor experiments

Mice were injected subcutaneously (s.c.) into the right lower back with EL4 or E.G7 thymoma cells (2×10^6), followed by intravenous injection of immature DCs and HBHA-treated DCs (1×10^6) pulsed with or without OVA (1 $\mu\text{g}/\text{mL}$) via the tail vein on days 1, 3, and 5 after tumor inoculation. Groups of tumor-bearing mice were treated with PBS, iDCs (untreated immature DCs), DCs-OVA (DCs pulsed with OVA peptide), or HBHA-DCs-OVA (HBHA-treated DCs pulsed with OVA peptide). Tumor size was measured every 2 days, and tumor mass was calculated as: $V = (2A \times B)/2$, where A is the length of the short axis and B is the length of the long axis.

Confocal laser scanning microscopy

Cells were permeabilized with 1% saponin for 3 minutes, stained with anti-mouse HBHA followed by Alexa568-conjugated anti-mouse IgG antibody overnight at 4°C, and then stained with Alexa488-conjugated anti-mouse TLR2 or TLR4/MD2 for 3 hours at room temperature. Cell morphology and fluorescence intensity were analyzed using a confocal laser scanning microscope (Zeiss LSM510 Meta). Images were acquired using the LSM510 Meta software and processed using the LSM image examiner.

Immunoprecipitation and immunoblotting

DCs (5×10^6) were incubated with 1 $\mu\text{g}/\text{mL}$ HBHA for 24 hours, and cell pellets were lysed with lysis buffer (10 mmol/L Tris-HCl, 150 mmol/L NaCl, 1.0 mmol/L EDTA, 1.0% NP-40, 2.0 mmol/L sodium orthovanadate, 1 mmol/L PMSF, 10 $\mu\text{g}/\text{mL}$ aprotinin, and 10 $\mu\text{g}/\text{mL}$ leupeptin). Total cell lysates were precleared with protein G Sepharose for 2 hours at 4°C. HBHA-associated proteins were immunoprecipitated by incubation with protein G Sepharose for 24 hours at 4°C after incubation with anti-goat as control Ab for anti-TLR2, anti-TLR2, anti-rat as control Ab for anti-TLR4, or anti-TLR4 Abs for 1 hour at 4°C. Samples were eluted, and immunoblot analysis was performed using an anti-HBHA mAb.

Antigen uptake quantification

Ag uptake was performed as recently described (14). Briefly, DCs (2×10^5) were equilibrated at 37°C or 4°C for 30 minutes and pulsed with 1 mg/mL FITC-conjugated dextran for 45 minutes, and then the action was stopped with cold staining buffer. Washed cells were stained with PE-conjugated anti-CD11c and analyzed using a FACSCalibur flow cytometer.

In vitro and in vivo migration of DCs

In vitro chemotaxis was performed as previously reported (21). For the *in vivo* migration test, DCs were labeled with 0.5 $\mu\text{mol}/\text{L}$ carboxyfluorescein diacetate succinimidyl ester (CFSE; Molecular Probes). Labeled cells (1×10^6) were

injected s.c. in the hind-leg footpad. Popliteal lymph nodes (LNs) were removed 72 hours later, mechanically disaggregated, and treated with collagenase A (1 mg/mL; Boehringer Mannheim) and DNase (0.4 mg/mL; Roche) for 30 minutes. The enzymatically treated cell suspension was evaluated for the percentage of CFSE⁺ DCs by FACScan (Becton Dickinson).

In vivo imaging

Nude mice were preinjected with TNF- α in the hind-leg footpad (30 ng/leg). A total of 1×10^6 labeled DCs in 50 μL PBS was injected s.c. in the hind-leg footpad. After 2 days, mice were anesthetized with an intramuscular (i.m.) injection of 100 $\mu\text{L}/\text{kg}$ zoletil 50 solution (Virbac Korea). *In vivo* imaging was performed using the Maestro *in vivo* imaging system (CRI, ex = 797 nm; em = 830 nm long-pass).

Mixed lymphocyte reaction

OVA-specific CD8⁺ T cells, derived from C57BL/6 OT-1 TCR transgenic mice, were negatively selected using a mouse CD8⁺ T-cell kit (Miltenyi Biotec). Mixed lymphocyte reaction (MLR) was performed as recently described (22).

ELISA for IFN- γ and IL-2

BALB/c mice were injected with PBS, untreated DCs, DCs-pulsed with OVA₂₅₇₋₂₆₄, or HBHA-treated DCs-pulsed with OVA₂₅₇₋₂₆₄ on days 1 and 7. Seven days following the final injection, splenocytes (2×10^6 per well) were isolated and restimulated for 24 hours with 10 $\mu\text{g}/\text{mL}$ OVA₂₅₇₋₂₆₄, and the culture supernatant was used for the detection of IFN- γ and IL-2 by using ELISA.

In vivo CTL assay

C57BL/6 mice were injected with PBS, untreated DCs, DCs-pulsed with OVA₂₅₇₋₂₆₄, or HBHA-treated DCs-pulsed with OVA₂₅₇₋₂₆₄ on days 1 and 7. At the 7 days after last immunization, spleen cells from syngeneic mice were red blood cell lysed followed by pulsing with or without 10 $\mu\text{g}/\text{mL}$ OVA₂₅₇₋₂₆₄ for 45 minutes at 37°C. Then, the OVA₂₅₇₋₂₆₄ pulsed and unpulsed populations were loaded with either 5 μM (high) or 0.5 μM (low) carboxyfluorescein succinimidyl ester (CFSE; Molecular Probe) at 37°C for 10 minutes. The 2 cell populations were mixed 1:1 before tail vein injection to the immunized mice (10^7 cells per mouse). At 4 hours after injection, spleens from recipient mice were isolated and single cell suspensions were prepared prior to flow cytometric analysis using a FACScan (Becton Dickinson). The number of CFSE^{high} and CFSE^{low} population were determined and the *in vivo* OVA-specific lysis percentage was enumerated [24] A.M. Byers, C.C. Kemball, J.M. Moser and A.E. Lukacher, Cutting edge, *J Immunol* **171** (2003), pp. 17-21. View Record in Scopus | Cited By in Scopus (52).

Statistical analysis

All experiments were repeated at least 3 times. The levels of significance for comparison between samples were determined by Tukey's multiple comparison test by using GradPad InStat software (Ver 3.05, GraphPad). The data in the graphs are expressed as the mean \pm SEM. Datasets of survival curves were analyzed by the Kaplan-Meier log-rank test.

Results

HBHA induces DC maturation

Soluble recombinant HBHA was expressed in *M. smegmatis* and characterized. Endotoxin levels in HBHA were undetectable (≤ 0.01 ng/mg; data not shown). The molecular mass of HBHA was approximately 29 kDa. The purity of HBHA was first assessed by sodium dodecyl SDS-PAGE, immunoblotting with an antihistidine Ab (Fig. 1A). In addition, the purity of rHBHA was quantified by Quantity-one software (Bio-Rad). The purity of HBHA was calculated by percentage of HBHA band against intensity/mm² of the entire protein bands. The rHBHA revealed 84 and 96% purity after using Ni-NTA column only (left panel) and Ni-NTA followed by P11 column (right panel), respectively when 20 μ g of each protein were assessed in silver nitrate staining (Supplementary Fig. 1). Apoptosis in DC cultures exposed to HBHA up to 1 μ g/mL did not change significantly, as detected by Annexin V and PI staining (Fig. 1B).

To investigate whether HBHA induces DC maturation, we measured the expression of DC maturation markers involved in Th activation, such as CD40, CD80, CD86, major histocompatibility complex (MHC) classes I and II by flow cytometry. LPS served as a positive control. HBHA strongly induced the expression of various surface molecules in a dose-dependent manner (Fig. 1C).

We then tested whether HBHA-treated DCs produce pro- or antiinflammatory cytokines required for a Th response. DCs secreted IL-12 and IL-10, which stimulate the proliferation and development of Th1 and Th2 cells, respectively (23). The levels of IL-12 p40/p70 production in HBHA-treated DCs were significantly ($P < 0.05$ – 0.001) greater than those produced by untreated DCs (Fig. 1D). ELISA studies also revealed high levels of IL-12p70 in the supernatant of HBHA-treated DCs (Fig. 1E).

We also measured the production of IL-10, a pleiotropic cytokine that inhibits DC function and Th1 responses (24). Interestingly, unlike LPS, HBHA does not induce IL-10 in DCs (Fig. 1D and 1E). In addition, HBHA-treated DCs showed an enhanced secretion of proinflammatory cytokines (IL-1 β , IL-6, and TNF- α) compared to untreated DCs (Fig. 1F). Similar to treatment with LPS, HBHA treatment significantly decreased the percentage of dextran⁺CD11c⁺ cells (Fig. 1G), as compared to untreated DCs. These results indicate that HBHA significantly enhances the phenotypic and functional maturation of DCs.

TLR4 signaling is required for HBHA-induced DC maturation

TLR2 and TLR4 have been reported to recognize *M. tuberculosis* in the context of activation and maturation of Ag-presenting cells *in vitro* (25). Therefore, we examined whether HBHA can be recognized by and acting through TLRs in DCs. To identify TLRs on DCs that interact with HBHA, wild type (WT), TLR2^{-/-}, and TLR4^{-/-} DCs were stimulated with HBHA, and HBHA on cell surface was detected with an Alexa568-conjugated anti-HBHA mAb (Fig. 2A and B). Anti-HBHA bound to the cell surface of WT, TLR2^{-/-} DCs, but not

TLR4^{-/-} DCs. To confirm the interaction between HBHA and TLR, we performed immunoprecipitation studies with TLR2 or TLR4 and HBHA in DCs. HBHA bound to TLR4 but not TLR2 (Fig. 2C). This observation was also confirmed by confocal microscopy. As expected, co-localization of HBHA and TLR4 but not TLR2 was detected (Fig. 2D).

To test the ability of HBHA to activate DCs via TLR4, we measured the expression of surface molecules and proinflammatory cytokine (IL-12 p70, TNF- α , IL-6, and IL-1 β) production in HBHA-treated WT, TLR2^{-/-}, or TLR4^{-/-} DCs. The expression of surface molecules (Fig. 2E) and proinflammatory cytokine secretion (Fig. 2F) were enhanced in WT or TLR2^{-/-} DCs by HBHA. In contrast, these effects were strongly diminished in TLR4^{-/-} DCs indicating that HBHA is an agonist for TLR4 in DCs.

TLR4 signals via the MyD88- and TRIF-dependent pathways (26). To investigate the importance of the MyD88- and TRIF-dependent pathways in HBHA-induced cytokine production by DCs, we compared DC-based cytokine production in WT, MyD88^{-/-} and TRIF-deficient mice. HBHA-induced production of IL-1 β , IL-6, and TNF- α was significantly reduced in the absence of MyD88 and TRIF (Fig. 2G). Our results suggest that MyD88 and TRIF are crucial for an optimal HBHA-induced cytokine response. Furthermore, proteinase K- or heat-treated HBHA lost its activity to stimulate IL-1 β production in DCs. However, HBHA was resistant to polymyxin B treatment, indicating that LPS contamination was not responsible for the observed effects (Supplementary Fig. 2).

TLR9 signaling is not required for HBHA-induced DC activation

TLR activation and signal transduction such as TLRs1, 2, 4, 5, and 6 are modulated by subcellular compartmentalization of receptors and downstream signaling components (27), and the intracellular localization of nucleic acid-sensing TLRs such as TLRs3, 7, and 9 appears to facilitate self versus nonself discrimination (28). Recent study has suggested that DNA derived from *M. tuberculosis* induces proinflammatory cytokines via TLR9-dependent pathway in macrophages and DCs (29). Thus, we decided to determine whether TLR9 affected to the HBHA-induced DC maturation. We showed that HBHA did not bind to TLR9^{-/-} DC (Fig. 3A) and TLR9 deficiencies had no effect on the level of surface molecules (Fig. 3B) and proinflammatory cytokines (Fig. 3C). These results provided the evidence that HBHA is an efficient TLR4 agonist.

HBHA enhances DC migration

To investigate whether HBHA affects DC migration, we measured the CCR7 expression in DCs. The CCR7 expression was upregulated in HBHA-treated DCs, similar to the level of LPS-treated DCs (Fig. 4A). Next, we analyzed the migratory capacity of DCs using a transwell migration assay chamber. HBHA increased the migratory capacity of DCs in response to CCL19 *in vitro* (Fig. 4B).

We also observed an increase in the number of CFSE-positive HBHA-treated DCs in the draining LN compared to that of CFSE-positive HBHA-untreated DCs *in vivo* (Fig. 4C). The migratory capacity of HBHA was further analyzed by

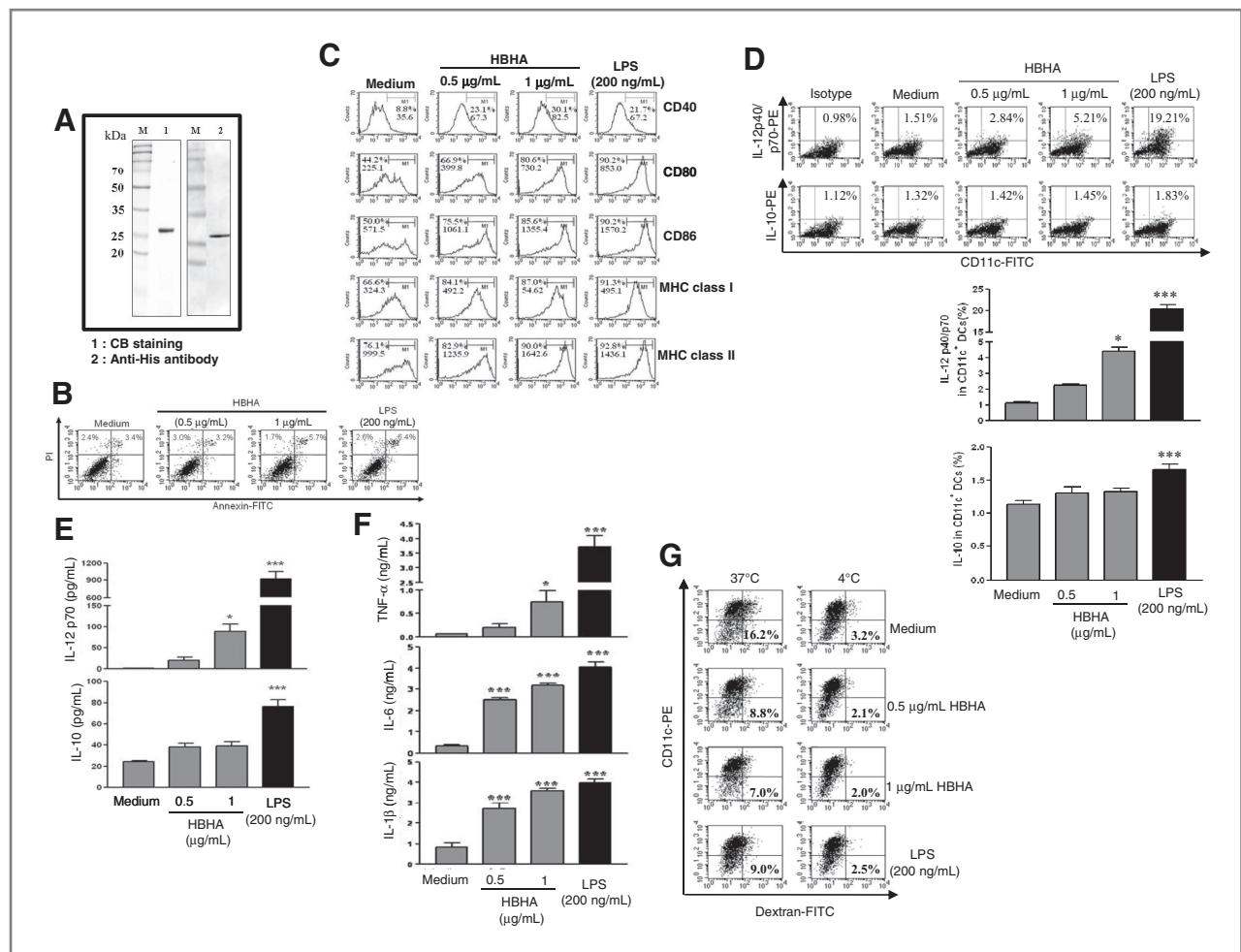


Figure 1. HBHA induces phenotypical and functional maturation of DCs. **A**, recombinant HBHA was purified by using an NTA resin, subjected to SDS-PAGE, and analyzed by Coomassie blue (CB) staining and immunoblot assay using antihistidine antibody. DCs were treated with the indicated concentrations of HBHA and LPS for 24 hours. **B**, DCs were stained with AnnexinV⁺ and PI⁺, and analyzed by flow cytometry. Results are representative of 4 separate experiments with similar results. **C**, flow cytometry was used to analyze the expression of surface molecules on CD11c⁺-gated cells. The mean fluorescence intensity (MFI) and percentage of positive cells are shown for each panel. **D**, dot plots of intracellular IL-12p40/p70 and IL-10 in CD11c⁺ DCs. The percentage of positive cells is shown in each panel. Bar graphs show the percentage (mean ± SEM) of IL-12p40/p70 and IL-10 in CD11c⁺ cells representing 4 independent experiments. *, $P < 0.05$ and ***, $P < 0.001$ compared to untreated DCs. **(E)** Production of IL-12p70 and IL-10 in HBHA-treated DCs were measured by using ELISA. The mean ± SEM values represent 3 independent experiments. *, $P < 0.05$ and ***, $P < 0.001$ compared to untreated DCs. **(F)** TNF- α , IL-6, and IL-1 β production in HBHA-treated DCs was analyzed by using the respective ELISA. The mean ± SEM values represent 3 independent experiments. *, $P < 0.05$ and ***, $P < 0.001$ compared to untreated DCs. **G**, endocytic activity of HBHA-treated versus untreated DCs. Endocytic activity at 37°C or 4°C was assessed by flow cytometry analysis as dextran-FITC uptake. The percentages of dextran-FITC⁺ CD11c⁺ cells are indicated.

using an *in vivo* image system. NEO-LIVE-labeled HBHA-untreated DCs were detected in the footpad, but not in the popliteal LN. In contrast, a remarkably strong fluorescence signal was detected in the popliteal LN (arrow) of mice injected with HBHA- or LPS-treated DCs (Fig. 4D). Overall, these results demonstrate that HBHA promotes DC migration *in vitro* and *in vivo*.

HBHA induces the activation of CD4⁺ and CD8⁺ T cells through TLR4-mediated DC activation

To precisely characterize HBHA activity on the interaction between DCs and T cells, we performed a syngeneic MLR assay

using OT-I T-cell receptor (TCR) transgenic CD8⁺ T cells, which express a TCR specific for the MHC class I-restricted OVA peptide 257–264 Ag (OVA_{257–264}) in DCs (30). HBHA-treated DCs pulsed with OVA_{257–264} elevated the cluster formation compared to untreated control DCs pulsed with OVA_{257–264} (Supplementary Fig. 3). Additionally, transgenic CFSE-labeled OVA-specific CD8⁺ T cells co-cultured with HBHA-treated DCs pulsed with OVA_{257–264} proliferated to a greater extent than did T cells co-cultured with untreated DCs pulsed with OVA_{257–264} (Fig. 5A). These results demonstrate that HBHA is a potent immunostimulator for T cells through DC activation. We then investigated the IFN- γ production in

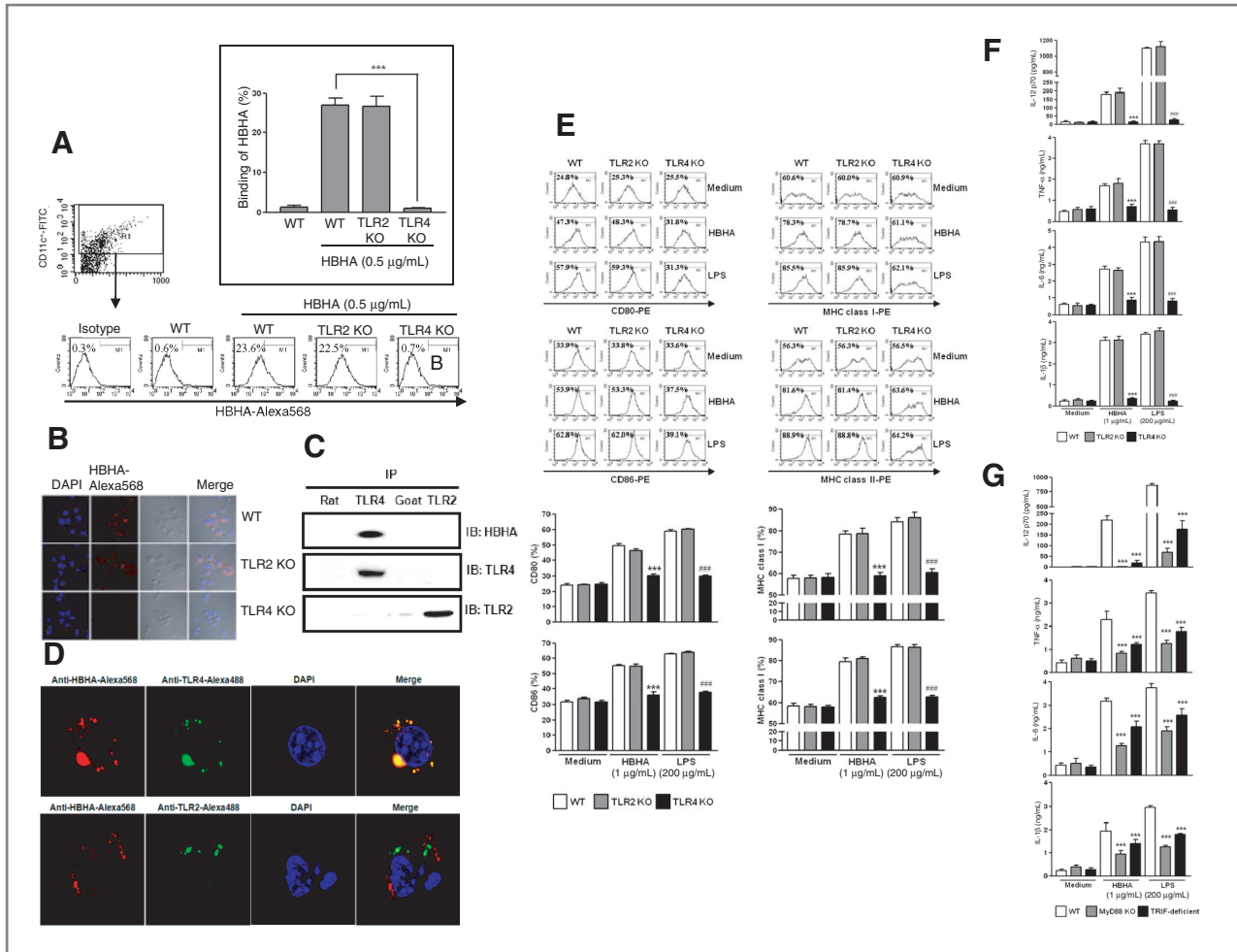


Figure 2. HBHA binds to TLR4, but not TLR2, and induces the activation of DCs. **A**, BMDCs derived from WT, TLR2^{-/-}, and TLR4^{-/-} mice were treated with HBHA (0.5 μg/mL) for 1 hour and stained with an Alexa568-conjugated anti-HBHA mAb. The percentage of positive cells is shown in each panel. Bar graphs show the mean ± SEM of percentage of HBHA-Alexa568 in CD11c⁺ cells representing 3 independent experiments. ***, *P* < 0.001 compared to HBHA treated WT DCs. **B**, fluorescence intensities of anti-HBHA binding to HBHA-treated DCs. DCs derived from WT, TLR2^{-/-}, and TLR4^{-/-} mice were treated with HBHA (0.5 μg/mL) for 1 hour, fixed, and stained with DAPI and an Alexa568-conjugated anti-HBHA mAb. **C**, immunoprecipitation (IP) with anti-TLR4 or -TLR2 antibodies and immunoblotting (IB) with anti-HBHA. DCs were treated with HBHA (1 μg/mL) for 24 hours. The cells were harvested, and cell lysates (1 mg) were IP with anti-rat IgG, anti-TLR2, anti-goat IgG, or anti-TLR4, and proteins were visualized by immunoblotting with anti-HBHA, -TLR4, or -TLR2 Abs. **D**, DCs were treated with HBHA (1 μg/mL) for 24 hours, fixed, and stained with Alexa568-conjugated mouse anti-HBHA mAb and Alexa488-conjugated mouse anti-TLRs Abs. Fluorescence signal indicates colocalization of HBHA and TLRs on DCs. **E**, histograms showing CD80, CD86, MHC I, or MHC II expression on HBHA-treated CD11c⁺-gated DCs derived from WT, TLR2^{-/-}, and TLR4^{-/-} mice. DCs derived from WT, TLR2^{-/-}, and TLR4^{-/-} mice were treated with HBHA (1 μg/mL) for 24 hours. The percentage of positive cells is shown for each panel. Bar graphs show the mean ± SEM of percentage of each surface molecule on CD11c⁺ cells representing 3 independent experiments. ***, ###*P* < 0.001, compared to HBHA (***)- or LPS (###)-treated WT DCs. **F**, DCs derived from WT, TLR2^{-/-}, and TLR4^{-/-} mice were treated with HBHA or LPS for 24 hours. IL-12 p70, TNF-α, IL-6, and IL-1β production in HBHA- or LPS-treated DCs derived from WT, TLR2^{-/-}, and TLR4^{-/-} mice was measured by using an ELISA. The mean ± SEM values represent 3 independent experiments. ***, ###*P* < 0.001, compared to HBHA (***)- or LPS (###)-treated WT DCs. **G**, DCs derived from WT, MyD88^{-/-}, and TRIF deficient mice were treated with HBHA (1 μg/mL) and LPS (200 ng/mL) for 24 hours. IL-12 p70, TNF-α, IL-6, and IL-1β production in HBHA- or LPS-treated DCs derived from WT, MyD88^{-/-}, and TRIF deficient mice was measured by using an ELISA. The mean ± SEM values represent 3 independent experiments. **, *P* < 0.01 and ***, *P* < 0.001, compared with WT cultures.

CD8⁺ T cells activated with HBHA-treated DCs. Syngeneic T cells primed with HBHA-treated DCs produced a significantly higher level of IFN-γ than those primed with untreated DCs (*P* < 0.05–0.01; Fig. 5C, left panel). Because DCs are also capable of inducing the polarization of naïve T cells, we evaluated the ability of HBHA-activated DCs to induce a Th1 phenotype from naïve CD4⁺ T cells. CD4⁺ splenic T cells from OT-II TCR transgenic mice were co-cultured with HBHA-

treated DCs pulsed with OVA_{323–339} also proliferated to greater extent than did T cells co-cultured with untreated DCs pulsed with OVA_{323–339} (Fig. 5B). Furthermore, analysis of culture supernatants showed that IFN-γ secretion increased in response to HBHA (Fig. 5C, right panel). Furthermore, we also measured the proliferation of T cells co-cultured with DCs pulsed with OVA whole protein instead of OVA peptide. Similar to OVA peptide pulsing, HBHA-treated DCs pulsed

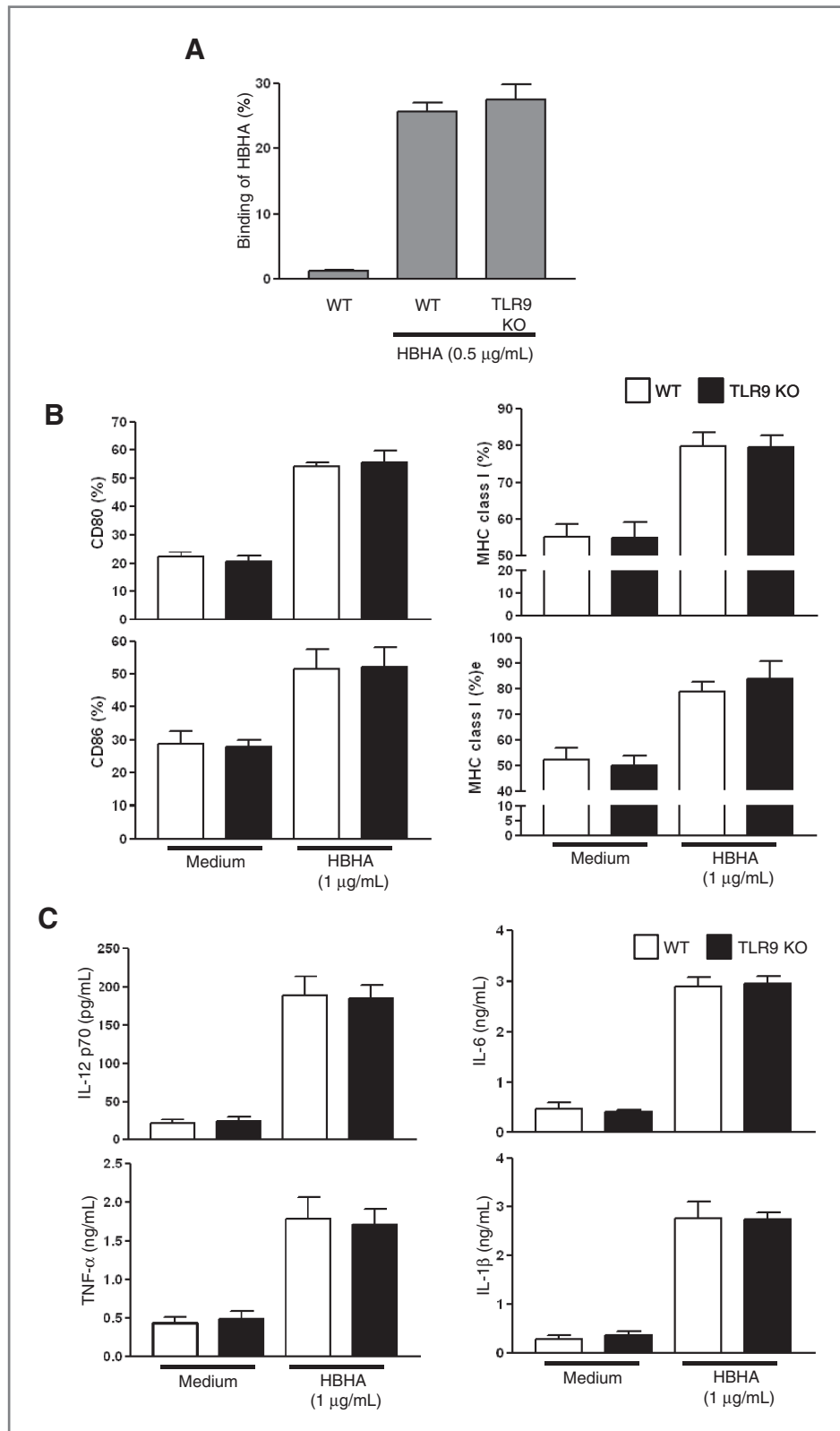
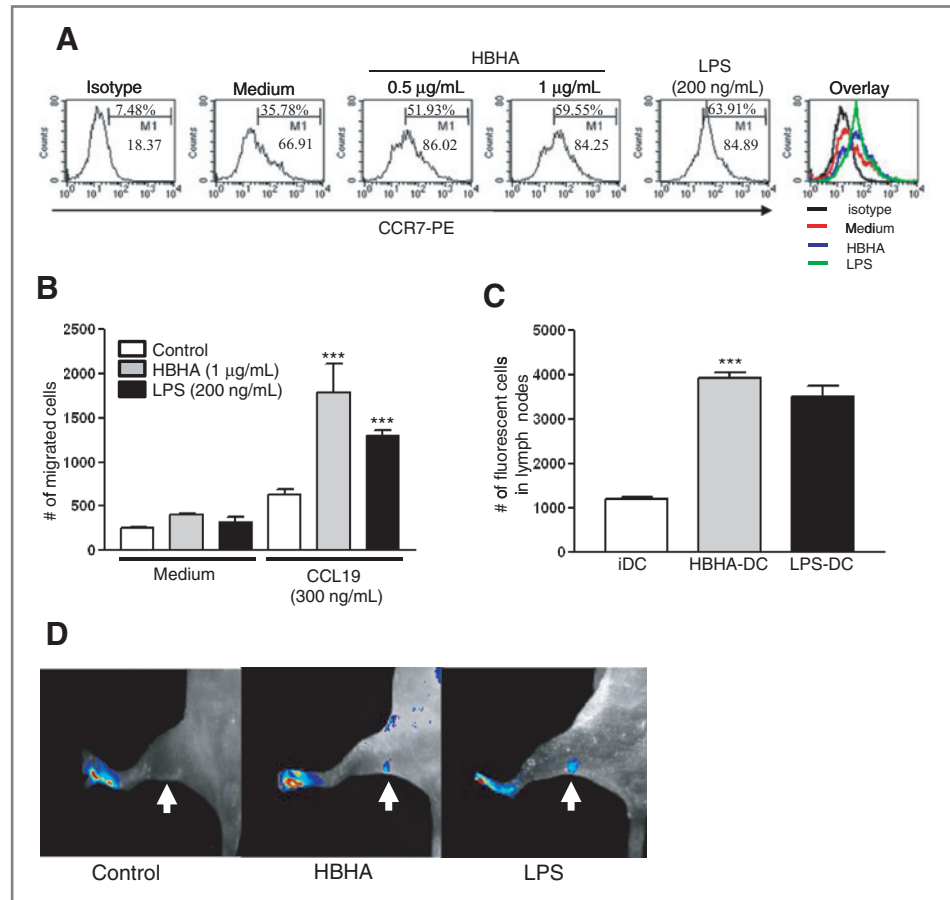


Figure 3. TLR9 does not affect HBHA-induced DC activation.

A. Bar graph showing anti-HBHA binding to HBHA-treated DCs. BMDCs derived from WT and TLR9^{-/-} mice were treated with HBHA (0.5 $\mu\text{g/mL}$) for 1 hour and stained with an Alexa568-conjugated anti-HBHA mAb. The mean \pm SEM values represent 3 independent experiments.

B. Histograms showing CD80, CD86, MHC I, or MHC II expression on HBHA-treated CD11c⁺-gated DCs derived from WT, TLR2^{-/-}, and TLR4^{-/-} mice. DCs derived from WT, TLR2^{-/-}, and TLR4^{-/-} mice were treated with HBHA (1 $\mu\text{g/mL}$) for 24 hours. Bar graphs show the mean \pm SEM of percentage of each surface molecule in CD11c⁺ cells represents 3 independent experiments. **(C)** IL-12 p70, TNF- α , IL-6, and IL-1 β production in HBHA- or LPS-treated DCs derived from WT and TLR9^{-/-} mice was measured by using an ELISA. The mean \pm SEM values represent 3 independent experiments.

Figure 4. HBHA enhances the migration of DCs *in vitro* and *in vivo*. **A**, DCs were treated with the indicated concentrations of HBHA and LPS for 24 hours. The percentage of CCR7⁺CD11c⁺ DCs was analyzed by flow cytometry. The number in each panel indicates the MFI of positive cells. **B**, DCs were treated with HBHA (1 μ g/mL) or LPS (200 ng/mL) for 24 hours and then subjected to an *in vitro* transwell chemotaxis assay with medium alone or medium containing CCL19 (300 ng/mL). ***, $P < 0.001$ compared to untreated DCs. **C**, Mice were injected subcutaneously to the hind-leg footpad with CFSE-labeled HBHA- or LPS-treated DCs and were recovered from popliteal LNs 72 hours later. CFSE-positive DCs were analyzed by flow cytometry. **D**, Images of mice injected with NEO-LIVE nanoparticle-labeled HBHA- or LPS-treated mature DCs. Mice were injected subcutaneously to the hind leg footpad with NEO-LIVE nanoparticle-positive DCs. NEO-LIVE nanoparticle-positive DCs were visualized using an *in vivo* imaging system.



with OVA whole protein also enhanced the proliferation of CD4⁺ and CD8⁺ T cells (Supplementary Fig. 4). These results suggest that HBHA directs T-cell differentiation toward a Th1 phenotype by inducing IL-12 production.

To test the capacity of HBHA to induce the interaction between DCs and T cells via TLR4, we performed a syngenic MLR assay using OT-I and OT-II TCR transgenic CD4⁺ and CD8⁺ T cells. HBHA-treated DCs derived from WT, TLR2^{-/-}, and TLR4^{-/-} mice pulsed with OVA₂₅₇₋₂₆₄ or OVA₃₂₃₋₃₃₉ and then co-cultured with transgenic CFSE-labeled OVA-specific CD8⁺ and CD4⁺ T cells. The proliferation of OT-I (Fig. 5D) and OT-II (Fig. 5E) cells were enhanced in HBHA- or LPS-treated WT and TLR2^{-/-} DCs pulsed with OVA peptide, whereas these effects were diminished in HBHA- or LPS-treated TLR4^{-/-} DCs pulsed with OVA peptide indicating that HBHA induce T-cell proliferation through TLR4-mediated DC activation.

HBHA enhances the antitumor efficacy

To show the therapeutic antitumor potential of HBHA, we used a murine tumor model in which EL4 or OVA-expressing E.G7 cells were implanted. On day 35 days following E.G7 tumor implantation, injection of DCs pulsed with OVA₂₅₇₋₂₆₄ significantly suppressed the E.G7 tumor growth (mean size,

5630.8 [97.3] mm³) compared to tumors in mice receiving PBS (mean size, 19,202.8 [277.4] mm³) or DCs alone (mean size, 16,949.4 [208.2] mm³; $P < 0.01$). Meanwhile, injection of OVA-pulsed DCs did not affect the EL4 tumor growth (Data not shown). Interestingly, E.G7 tumors in mice that received HBHA-treated DCs pulsed with OVA₂₅₇₋₂₆₄ were significantly smaller (mean size, 2,925.7 [60.1] mm³) than that in mice received DCs pulsed with OVA (Fig. 6A). Notably, only 20% of mice injected with OVA-pulsed DCs survived beyond 60 days following E.G7 tumor implantation as compared to over 50% survival of mice injected with HBHA-treated OVA-pulsed DCs. In contrast, all mice in the PBS and HBHA-untreated DCs-injected groups had a median survival of 34 days with no long-term survivors (Fig. 6B).

To test the engagement of TLR4 in the retardation of tumor growth by immunization with HBHA-treated DCs pulsed with OVA, E.G7 cells implanted mice were immunized with DCs pulsed with OVA₂₅₇₋₂₆₄ (DC-OVA), HBHA-treated WT DCs pulsed with OVA₂₅₇₋₂₆₄ [HBHA-DC(WT)-OVA], HBHA-treated TLR2^{-/-} DCs pulsed with OVA₂₅₇₋₂₆₄ [HBHA-DC(TLR2 KO)-OVA], or HBHA-treated TLR4^{-/-} DCs pulsed with OVA₂₅₇₋₂₆₄ [HBHA-DC(TLR4 KO)-OVA]. Although injection of HBHA-DC (WT)-OVA (mean size, 6,869.3 [753.4] mm³) and HBHA-DC (TLR2 KO)-OVA (mean size, 8,178.8 [664.7] mm³) significantly

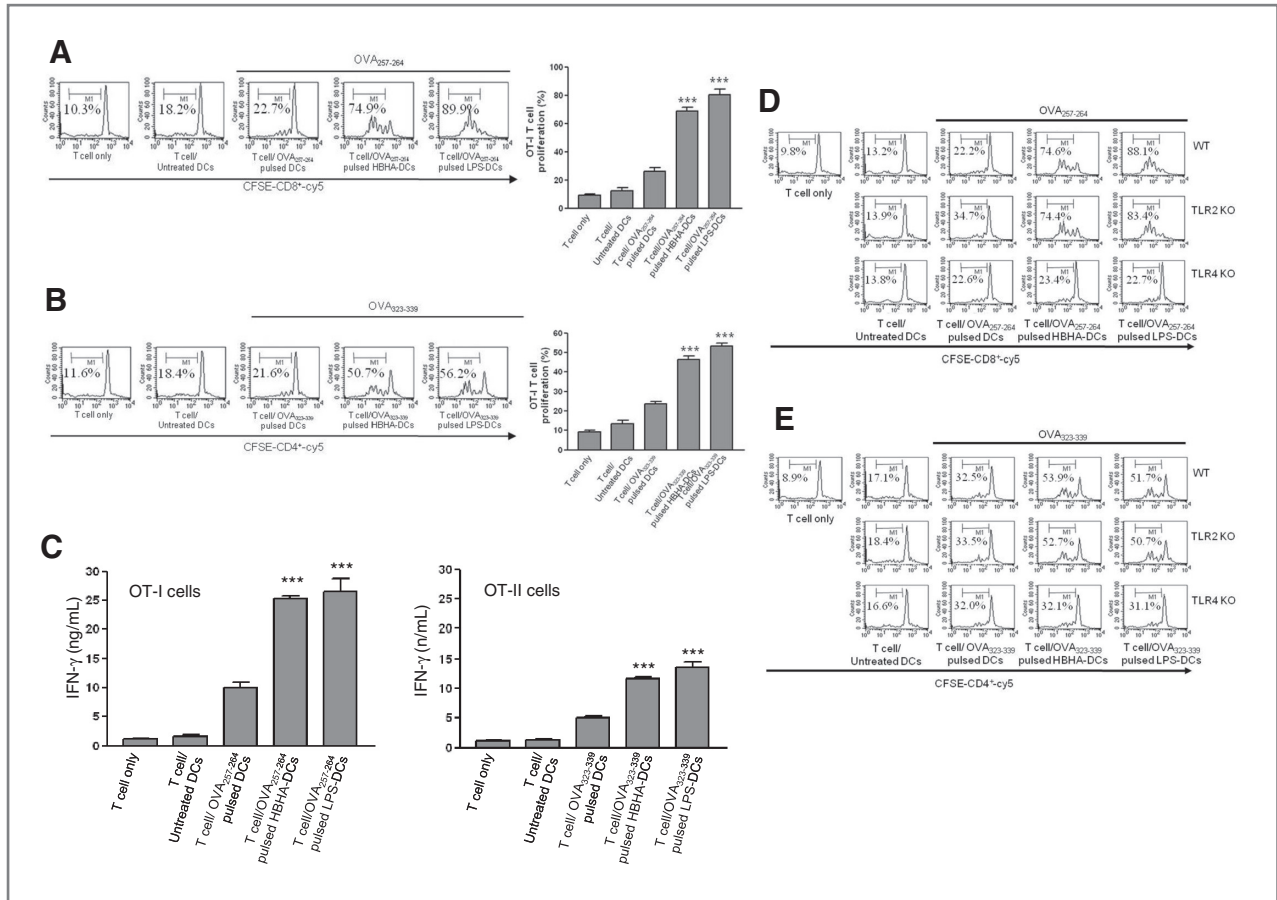


Figure 5. HBHA-treated DCs induce proliferation of T cells and a Th1 response via TLR4 signaling. **A**, Transgenic OVA-specific CD8⁺ T cells and **B**) transgenic OVA-specific CD4⁺ T cells were isolated, stained with CFSE, and co-cultured for 96 hours with DCs treated with HBHA or LPS and pulsed with **(A)** OVA₂₅₇₋₂₆₄ (1 μg/mL) for OVA-specific CD8⁺ T cells or **(B)** OVA₃₂₃₋₃₃₉ (1 μg/mL) for OVA-specific CD4⁺ T cells, respectively. T cells only and T cells co-cultured with untreated DCs served as controls. Then, the proliferation of **(A)** OT-I⁺ and **(B)** OT-II⁺ T cells was assessed by flow cytometry. Bar graphs show the percentage (mean ± SEM of 4 separate experiments) of **(A)** OT-I⁺ and **(B)** OT-II⁺ T-cell proliferation. ***, $P < 0.001$ compared to **(A)** T cell/OVA₂₅₇₋₂₆₄ pulsed or **(B)** T cell/OVA₃₂₃₋₃₃₉ pulsed DCs. **C**, The culture supernatants obtained from the condition described on the **A** and **B** were harvested after 24 hours and IFN-γ was measured by using an ELISA. The mean ± SEM values represent 4 independent experiments. *, $P < 0.05$ and **, $P < 0.01$ compared to T cell/OVA₂₅₇₋₂₆₄ pulsed DCs or T cell/OVA₃₂₃₋₃₃₉ pulsed DCs, respectively. Transgenic **(D)** OVA-specific CD8⁺ T cells (OT-I cells) or **(E)** OVA-specific CD4⁺ T cells (OT-II cells) were isolated, stained with CFSE, and co-cultured for 96 hours with DCs derived from WT, TLR2^{-/-}, and TLR4^{-/-} mice and pulsed with **(D)** OVA₂₅₇₋₂₆₄ (1 μg/mL) or **(E)** OVA₃₂₃₋₃₃₉ (1 μg/mL). Histograms showing **(D)** OT-I⁺ and **(E)** OT-II⁺ cell proliferation was assessed by flow cytometry.

suppressed the E.G7 tumor growth compared to tumors in mice receiving DC-OVA (mean size, 18,256.7 [803.3] mm³), injection of HBHA-DC(TLR4 KO)-OVA (mean size, 16,115.9 [971.0] mm³) did not suppress the E.G7 tumor growth (Fig. 6C). In addition, the survival rate was also significantly decreased in HBHA-DC(TLR4 KO)-OVA compared to mice receiving HBHA-DC(WT)-OVA ($P < 0.001$; Fig. 6D).

HBHA increases CTL activity in tumor-bearing mice via TLR4 signaling

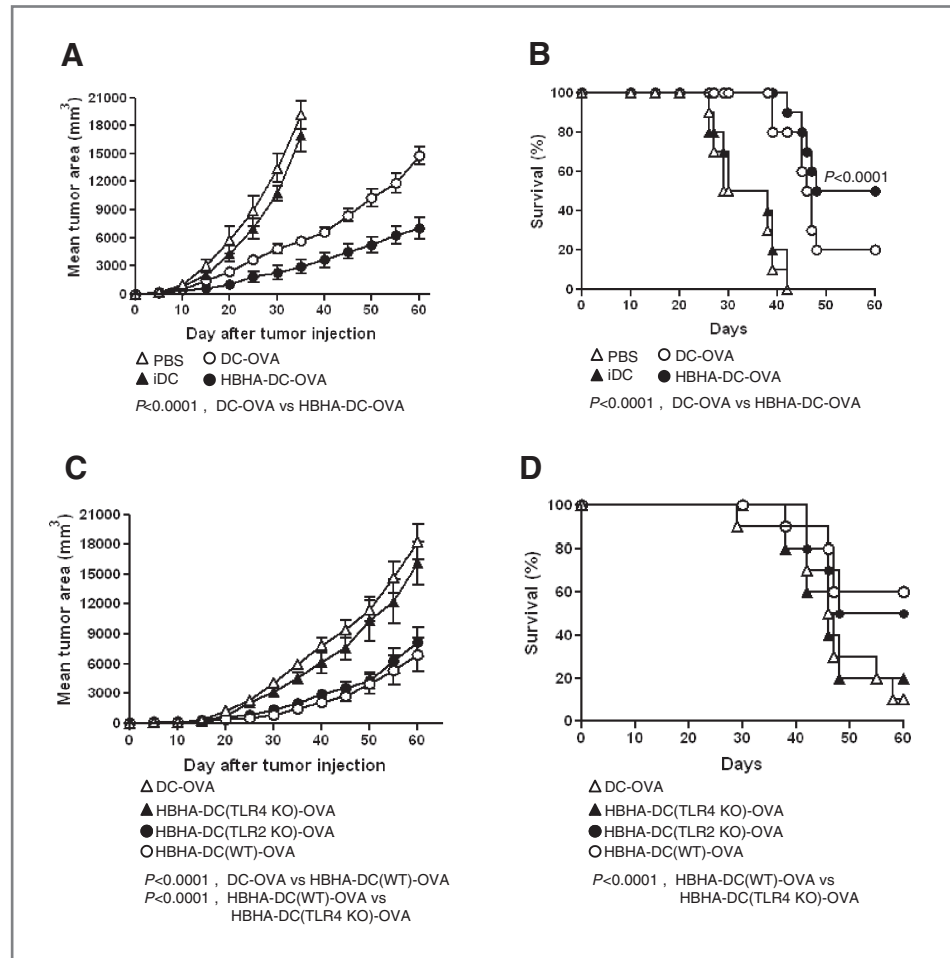
To further investigate the mechanism of tumor protection after HBHA-treated DC vaccination, we first sought to determine whether a humoral antitumor immune response was induced. Serum from E.G7 tumor implanted mice was collected at day 7 after final immunization with PBS, untreated DCs (iDC), DCs pulsed with OVA₂₅₇₋₂₆₄ (DC-OVA), or HBHA-treated

DCs pulsed with OVA₂₅₇₋₂₆₄ (HBHA-DC-OVA) and assessed for IgG2a production. The level of IgG2a was increased in tumor-bearing mice received with DC-OVA, whereas that was significantly ($P < 0.001$) enhanced in tumor-bearing mice received with HBHA-DC-OVA (Supplementary Fig. 5).

Next, to examine the *in vivo* cytolytic function of the memory T cells, mice were immunized with PBS, untreated DCs (iDC), DCs pulsed with OVA₂₅₇₋₂₆₄ (DC-OVA), or HBHA-treated DCs pulsed with OVA₂₅₇₋₂₆₄ (HBHA-DC-OVA) at days 1 and 7. At 7 days after the last immunization, the mice were injected with a mixture of syngeneic splenocytes pulsed with OVA₂₅₇₋₂₆₄ (CFSE^{hi}) or without OVA₂₅₇₋₂₆₄ (CFSE^{low}), and the elimination of OVA-pulsed splenocytes (CFSE^{hi}) was examined by flow cytometry.

In addition, a significantly high level of target cell lysis was observed in mice received HBHA-DC-OVA (79.3 [0.68]%)

Figure 6. Changes of tumor size and survival in mice that received HBHA-treated DCs pulsed with OVA₂₅₇₋₂₆₄ against E.G7 tumor challenge. C57BL/6 mice were challenged with subcutaneous injection of 2×10^6 E.G7 cells into the right flank area. A and B, mice were injected intravenously with PBS, untreated DC (iDC), DCs pulsed with OVA₂₅₇₋₂₆₄ (DC-OVA), or HBHA-treated DCs pulsed with OVA₂₅₇₋₂₆₄ (HBHA-DC-OVA; 1×10^6 cells) on days 1, 3, and 5 after the tumor challenge. C and D, mice were injected intravenously with DCs pulsed with OVA₂₅₇₋₂₆₄ (DC-OVA), HBHA-treated WT-DCs pulsed with OVA₂₅₇₋₂₆₄ [HBHA-DC(WT)-OVA], HBHA-treated TLR2 KO-DCs pulsed with OVA₂₅₇₋₂₆₄ [HBHA-DC(TLR2 KO)-OVA], or HBHA-treated TLR4 KO-DCs pulsed with OVA₂₅₇₋₂₆₄ [HBHA-DC(TLR4 KO)-OVA; 1×10^6 cells] on days 1, 3, and 5 after the tumor challenge. A and C, following tumor challenge, tumor growth was monitored by measuring the diameter of the tumor every 5 days for 60 days. $n = 10$ mice/group. B and D, survival of mice with E.G7 tumor challenge after injection of HBHA-treated DCs pulsed with OVA₂₅₇₋₂₆₄; $n = 10$ mice/group. P value was calculated by Kaplan-Meier log-rank test.



compared to those received PBS (0 [0.05]%), iDC (0.43 [0.15]%), or DC-OVA (49 [2.05]%; Fig. 7A). These results suggested that HBHA could be an important element in a cancer vaccine against OVA positive thymoma tumor by inducing killing activity to target cells.

To assess whether the lymphocytes induced by the HBHA-treated DCs pulsed with OVA₂₅₇₋₂₆₄ is able to produce the essential cytokine, we observed significantly higher levels of IFN- γ and IL-2 secretion when splenocytes from mice injected with HBHA-treated DCs pulsed OVA₂₅₇₋₂₆₄ (HBHA-DC-OVA) were restimulated with OVA₂₅₇₋₂₆₄, compared to those of splenocytes from mice injected with DCs pulsed with OVA₂₅₇₋₂₆₄ (DC-OVA; $P < 0.001$; Fig. 7B).

To test the engagement of TLR4 in the induction of CTL activity by immunization with HBHA-treated DCs pulsed with OVA, mice were immunized with PBS, untreated DCs (iDC), DCs pulsed with OVA₂₅₇₋₂₆₄ (DC-OVA), HBHA-treated WT DCs pulsed with OVA₂₅₇₋₂₆₄ [HBHA-DC(WT)-OVA], HBHA-treated TLR2^{-/-} DCs pulsed with OVA₂₅₇₋₂₆₄ [HBHA-DC(TLR2 KO)-OVA], or HBHA-treated TLR4^{-/-} DCs pulsed with OVA₂₅₇₋₂₆₄ [HBHA-DC(TLR4 KO)-OVA]. Target cell lysis in mice received HBHA-DC

(TLR4 KO)-OVA was significantly suppressed compared to mice received HBHA-DC(WT)-OVA (Fig. 7C). This data suggest that HBHA can modulate the CTL activity via TLR4-dependent pathway.

To further delineate the mechanism by which OVA-specific DC vaccination resulted in improved tumor retardation, we analyzed surface expression of CD62L and CD44, both of which have been implicated in cell migration to the site of Ag deposition (31), on CD8⁺ T cells in spleen. Using flow cytometry, we identified naive (CD62L^{high}CD44^{low}) and effector/memory cells (CD62L^{low}CD44^{high}). By day 7 after final immunization with HBHA-treated DCs-pulsed with OVA, CD8⁺ T cells in spleen showed significantly downregulated CD62L and upregulated CD44 expression when immunized with DCs pulsed with OVA (Fig. 7D).

Discussion

The immune system can recognize many tumor Ags however, the ability of tumors to evade the immune system suggests that host defense mechanism cannot effectively prevent some tumors. In an attempt to boost the antitumor

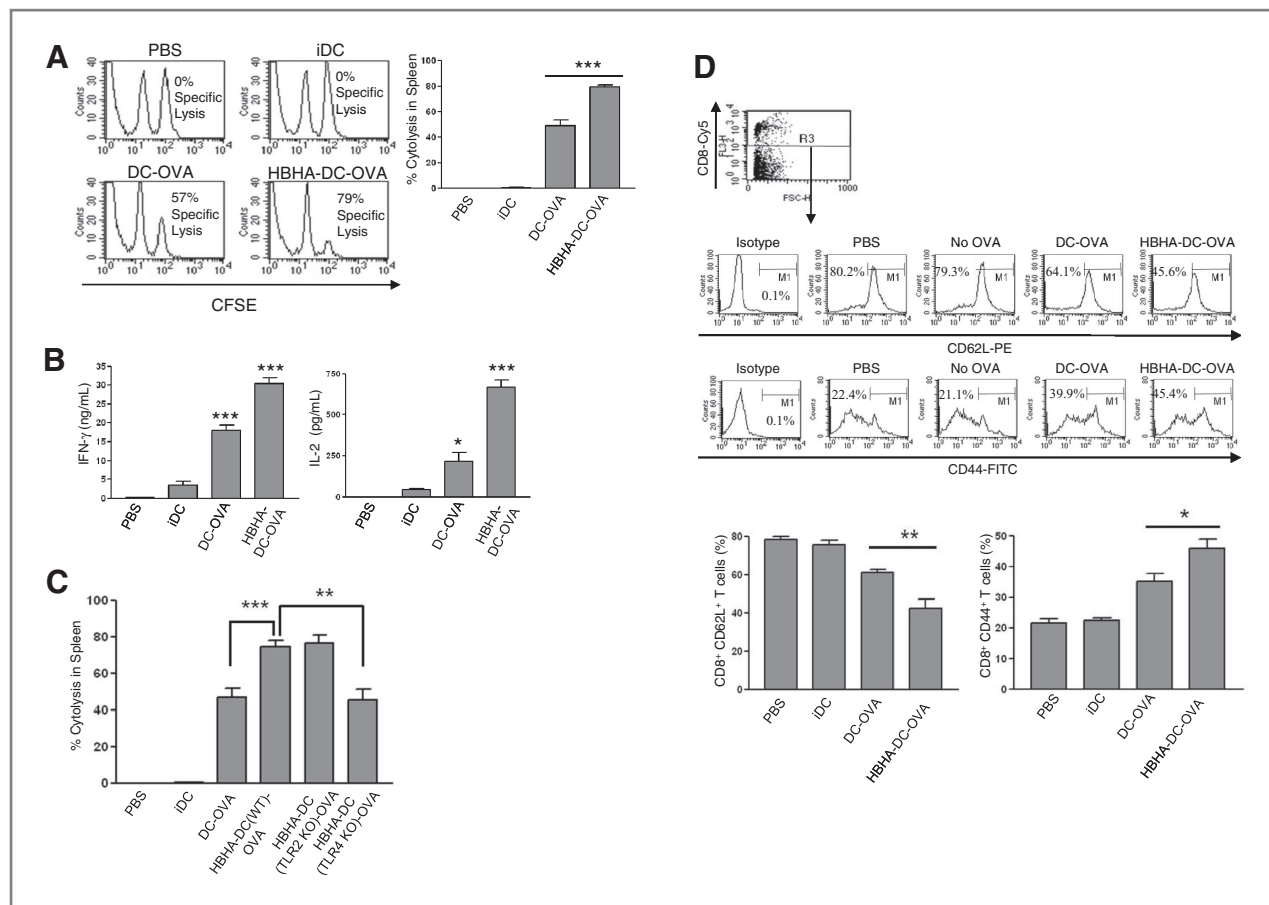


Figure 7. HBHA-treated DCs pulsed with OVA₂₅₇₋₂₆₄ enhance the activity of CTL and effector/memory T cells. **A**, *In vivo* CTL activity. C57BL/6 mice were primed with PBS, immature DCs (iDC), DCs pulsed with OVA₂₅₇₋₂₆₄ (DC-OVA), or HBHA-treated DCs pulsed with OVA₂₅₇₋₂₆₄ (HBHA-DC-OVA) on days 1 and 7. 7 days after boosting, CTL activity was determined by challenge with CFSE^{high} OVA₂₅₇₋₂₆₄-loaded splenocytes. Number indicates the percentage of specific killing. Bar graphs show the mean \pm SEM of percentage of specific killing represents 3 independent experiments. ***, $P < 0.001$. **B**, BALB/c mice were treated with immature DCs (iDC), DCs pulsed with OVA₂₅₇₋₂₆₄ (DC-OVA), or HBHA-treated DCs pulsed with OVA₂₅₇₋₂₆₄ (HBHA-DC-OVA) on days 1 and 7. 10 days after boosting, splenocytes were isolated and treated with 10 μ g/mL of OVA₂₅₇₋₂₆₄ for 24 hours. IL-2 and IFN- γ production was measured by an ELISA. The mean \pm SEM values represent 3 independent experiments. *, $P < 0.05$ and ***, $P < 0.001$, compared to T cells primed with untreated DCs. **C**, *In vivo* CTL activity. C57BL/6 mice were primed with PBS, immature DCs (iDC), DCs pulsed with OVA₂₅₇₋₂₆₄ (DC-OVA), HBHA-treated WT DCs pulsed with OVA₂₅₇₋₂₆₄ [HBHA-DC(WT)-OVA], HBHA-treated TLR2^{-/-} DCs pulsed with OVA₂₅₇₋₂₆₄ [HBHA-DC(TLR2 KO)-OVA], or HBHA-treated TLR4^{-/-} DCs pulsed with OVA₂₅₇₋₂₆₄ [HBHA-DC(TLR4 KO)-OVA] on days 1 and 7. 7 days after boosting, CTL activity was determined by challenge with CFSE^{high} OVA₂₅₇₋₂₆₄-loaded splenocytes. Bar graphs show the mean \pm SEM of percentage of specific killing represents 3 independent experiments. **, $P < 0.01$ and ***, $P < 0.001$. **(D)** C57BL/6 mice were challenged by subcutaneous injection of with E.G7 tumor cells into the right flank area. One and 7 days after tumor challenge, mice were injected intravenously with PBS, immature DCs, DCs-pulsed with OVA, or HBHA-treated DCs-pulsed with OVA. Splenocytes were isolated 7 days after final immunization and stained with anti-CD8 mAb, anti-CD69L, and anti-CD44 mAb. Histograms and bar graphs show CD62L⁺CD44⁺ T cells in spleen. Bar graphs show the percentage (mean \pm SEM) of CD8⁺CD62L⁺ (bottom left panel) and CD8⁺CD44⁺ (bottom right panel) T cells representing 3 independent experiments. *, $P < 0.05$ and ***, $P < 0.001$.

immunity, we focused on a DC-based antitumor immunotherapy using HBHA as an adjuvant.

DCs are the most potent APCs and versatile regulators of T lymphocyte responses (32, 33). Immature DCs capture Ags, process them into peptides, and present on the cell surface in association with MHC class I or II to prime CD8⁺ CTLs or CD4⁺ Th1 cells, respectively (32, 33). Immunization with *ex vivo* tumor Ag-loaded DCs is a promising tool for eliciting efficient antitumor immunity (34). This approach has been successfully used to vaccinate mice and to activate CTL responses in preclinical human trials (35–38).

In this study, we identified the novel properties of HBHA that HBHA can induce DC maturation via TLR4 activation. Importantly, HBHA improved the efficacy of the DC-based antitumor immunotherapy in mice by acting as an adjuvant. The evidence for these novel characteristics of HBHA includes: (1) increased expression of surface molecules and proinflammatory cytokines in HBHA-treated DCs; (2) reduced HBHA-induced DC activation in TLR4^{-/-} DCs but not in TLR2^{-/-} DCs; (3) increased migratory capacity of HBHA-treated DCs; and (4) significantly elevated OVA-specific CTL activity and suppression of tumor growth.

We showed that the interaction of HBHA with DCs inhibits the endocytic ability of DCs and induces the increased expression of surface molecules. Furthermore, HBHA-treated DCs enhanced primary syngeneic T-cell proliferation more efficiently than untreated DCs. HBHA-treated DCs also triggered the secretion of IL-1 β , IL-6, IL-12p70, and TNF- α . Because IL-12 is essential for Th1 polarization (39) HBHA might promote Th1 immune responses. Furthermore, HBHA-treated DCs triggered the IFN- γ production in CD4⁺ and CD8⁺ T cells, which is another feature of Th1 responses. These findings indicate that the antitumor effect of HBHA-treated DCs is closely related to the increased production of IFN- γ .

In addition, to investigate the adjuvant activity of HBHA, we administered the model adjuvant OVA alone or in combination with HBHA. It is well documented that the type of IgG subclass reflects the pattern of immune responses in mice: IgG2a for Th1 and IgG1 for Th2 (40). OVA alone significantly enhanced IgG1 responses (Supplementary Fig. 6). Interestingly, however, HBHA dramatically augmented IgG2a (Th1-associated) but not IgG1 (Th2-associated) responses to OVA. Thus, HBHA is a potent adjuvant triggering Th1-mediated humoral immune responses.

In addition, HBHA induced the CCR7 expression, which is critical for the migration of DCs from the periphery to T-cell-rich regions of secondary lymphoid organs (41, 42). Importantly, HBHA enhanced the migration of DCs toward CCL19 *in vitro* and resulted in the draining of LNs *in vivo*. HBHA has multiple effects on DC function, indicating that it can be an effective adjuvant for DC-based antitumor immunotherapies.

TLRs are expressed by many immune cells and play a key role in innate and adaptive immune responses (43). TLR4 agonists have important immunoregulatory applications, such as adjuvants for vaccines in antitumor therapies (44). Moreover, adjuvant studies for cancer treatment have recently been focused on TLR4 agonist because the signal through these receptors are mediated by either MyD88- and TRIF-dependent pathway and appear to be especially powerful immunopotentiators (45). Although LPS, the most studied and well-characterized TLR4 agonist, showed highly effective adjuvancy in both experimental and clinical setting (46), it is not suitable

for clinical use due to its toxicity in humans. Thus, novel TLR4 agonists will be extremely beneficial as vaccine adjuvants in antitumor therapy.

Some *M. tuberculosis* proteins have a significant immunostimulatory potential. Both TLR2 and TLR4 mediate *M. tuberculosis*-induced intracellular signaling in APCs (47). Furthermore, several molecules from *M. tuberculosis* have now been identified as TLR2 agonists and are known to induce APC activation (48, 49). However, TLR4 agonists have not yet been identified. We showed that HBHA directly binds TLR4 and activates TLR4-mediated MyD88 and TRIF signaling, leading to the expression of surface molecules and proinflammatory cytokines' production by DCs (Fig. 2).

On the basis of the results described herein, we suggest that HBHA could be used for DC-based antitumor immunotherapies. It is obvious that immunotherapy using HBHA for tumor treatment has not yet been explored in detail including safety issue. However, because of its ability to stimulate DCs, which then further activate T cells that are able to lyse tumor cells and suppress tumor growth, we propose HBHA as a novel and potent adjuvant with potential applications in antitumor immunotherapy.

Disclosure of Potential Conflicts of Interest

No potential conflicts of interest were disclosed.

Acknowledgments

We thank Dr. Clifton E. Barry III and Dr. Yong-Soo Bae for critical reading of the manuscript and discussions.

Grant Support

This study was supported by a grant of the Korea Healthcare Technology R&D Project, Ministry for Health Welfare & Family Affairs, Republic of Korea (A091047) and by the National Research Foundation of Korea (NRF) grant funded by the Korea government (MEST; 2010-0008728).

The costs of publication of this article were defrayed in part by the payment of page charges. This article must therefore be hereby marked *advertisement* in accordance with 18 U.S.C. Section 1734 solely to indicate this fact.

Received September 23, 2010; revised February 8, 2011; accepted February 19, 2011; published OnlineFirst March 2, 2011.

References

- Banchereau J, Palucka AK. Dendritic cells as therapeutic vaccines against cancer. *Nat Rev Immunol* 2005;5:296-306.
- Figdor CG, de Vries IJ, Lesterhuis WJ, Melief CJ. Dendritic cell immunotherapy: mapping the way. *Nat Med* 2004;10:475-80.
- Felzmann T, Gadner H, Holter W. Dendritic cells as adjuvants in antitumor immune therapy. *Onkologie* 2002;25:456-64.
- Matijevic T, Pavelic J. Toll-like receptors: cost or benefit for cancer? *Curr Pharm Des* 16:1081-90.
- Medzhitov R, Janeway CA Jr. Innate immunity: the virtues of a nonclonal system of recognition. *Cell* 1997;91:295-98.
- Carter WA, Strayer DR, Hubbell HR, Brodsky I. Preclinical studies with Ampligen (mismatched double-stranded RNA). *J Biol Response Mod* 1985;4:495-502.
- Beutler B. TLR4 as the mammalian endotoxin sensor. *Curr Top Microbiol Immunol* 2002;270:109-20.
- Agrawal S, Agrawal A, Doughty B, Gerwitz A, Blenis J, Van Dyke T, et al. Cutting edge: different Toll-like receptor agonists instruct dendritic cells to induce distinct Th responses via differential modulation of extracellular signal-regulated kinase-mitogen-activated protein kinase and c-Fos. *J Immunol* 2003;171:4984-9.
- Gorden KB, Gorski KS, Gibson SJ, Kedl RM, Kieper WC, Qiu X, et al. Synthetic TLR agonists reveal functional differences between human TLR7 and TLR8. *J Immunol* 2005;174:1259-68.
- Peng G, Guo Z, Kuniwa Y, Voo KS, Peng W, Fu T, et al. Toll-like receptor 8-mediated reversal of CD4+ regulatory T cell function. *Science* 2005;309:1380-4.
- Sun S, Kishimoto H, Sprent J. DNA as an adjuvant: capacity of insect DNA and synthetic oligodeoxynucleotides to augment T cell responses to specific antigen. *J Exp Med* 1998;187:1145-50.

12. Grange JM, Bottasso O, Stanford CA, Stanford JL. The use of mycobacterial adjuvant-based agents for immunotherapy of cancer. *Vaccine* 2008;26:4984–90.
13. Hope JC, Thom ML, McCormick PA, Howard CJ. Interaction of antigen presenting cells with mycobacteria. *Vet Immunol Immunopathol* 2004;100:187–95.
14. Lee JS, Shin SJ, Collins MT, Jung ID, Jeong YI, Lee CM, et al. Mycobacterium avium subsp. paratuberculosis fibronectin attachment protein activates dendritic cells and induces a Th1 polarization. *Infect Immun* 2009;77:2979–88.
15. Loch C, Hougardy JM, Rouanet C, Place S, Mascart F. Heparin-binding hemagglutinin, from an extrapulmonary dissemination factor to a powerful diagnostic and protective antigen against tuberculosis. *Tuberculosis (Edinb)*. 2006;86:303–9.
16. Pethe K, Alonso S, Biet F, Delogu G, Brennan MJ, Loch C, et al. The heparin-binding haemagglutinin of *M. tuberculosis* is required for extrapulmonary dissemination. *Nature* 2001;412:190–4.
17. Temmerman S, Pethe K, Parra M, Alonso S, Rouanet C, Pickett T, et al. Methylation-dependent T cell immunity to Mycobacterium tuberculosis heparin-binding hemagglutinin. *Nat Med* 2004;10:935–41.
18. Delogu G, Bua A, Pusceddu C, Parra M, Fadda G, Brennan MJ, et al. Expression and purification of recombinant methylated HBHA in Mycobacterium smegmatis. *FEMS Microbiol Lett* 2004;239:33–9.
19. Shin AR, Lee KS, Lee JS, Kim SY, Song CH, Jung SB, et al. Mycobacterium tuberculosis HBHA protein reacts strongly with the serum immunoglobulin M of tuberculosis patients. *Clin Vaccine Immunol* 2006;13:869–75.
20. Jung ID, Lee MG, Chang JH, Lee JS, Jeong YI, Lee CM, et al. Blockade of indoleamine 2,3-dioxygenase protects mice against lipopolysaccharide-induced endotoxin shock. *J Immunol* 2009;182:3146–54.
21. Jung ID, Lee JS, Kim YJ, Jeong YI, Lee CM, Lee MG, et al. Sphingosine kinase inhibitor suppresses dendritic cell migration by regulating chemokine receptor expression and impairing p38 mitogen-activated protein kinase. *Immunology* 2007;121:533–44.
22. Jeong YI, Kim SW, Jung ID, Lee JS, Chang JH, Lee CM, et al. Curcumin suppresses the induction of indoleamine 2,3-dioxygenase by blocking the Janus-activated kinase-protein kinase Cdelta-STAT1 signaling pathway in interferon-gamma-stimulated murine dendritic cells. *J Biol Chem* 2009;284:3700–8.
23. Trinchieri G. Interleukin-12 and the regulation of innate resistance and adaptive immunity. *Nat Rev Immunol* 2003;3:133–46.
24. Trinchieri G. Interleukin-10 production by effector T cells: Th1 cells show self control. *J Exp Med* 2007;204:239–43.
25. Means TK, Wang S, Lien E, Yoshimura A, Golenbock DT, Fenton MJ. Human toll-like receptors mediate cellular activation by Mycobacterium tuberculosis. *J Immunol* 1999;163:3920–7.
26. Yamamoto M, Sato S, Hemmi H, Hoshino K, Kaisho T, Sanjo H, et al. Role of adaptor TRIF in the MyD88-independent toll-like receptor signaling pathway. *Science* 2003;301:640–3.
27. Barton GM, Kagan JC. A cell biological view of Toll-like receptor function: regulation through compartmentalization. *Nat Rev Immunol* 2009;9:535–42.
28. Barton GM, Kagan JC, Medzhitov R. Intracellular localization of Toll-like receptor 9 prevents recognition of self DNA but facilitates access to viral DNA. *Nat Immunol* 2006;7:49–56.
29. Bafica A, Scanga CA, Feng CG, Leifer C, Cheever A, Sher A. TLR9 regulates Th1 responses and cooperates with TLR2 in mediating optimal resistance to Mycobacterium tuberculosis. *J Exp Med* 2005;202:1715–24.
30. Hogquist KA, Jameson SC, Heath WR, Howard JL, Bevan MJ, Carbone FR. T cell receptor antagonist peptides induce positive selection. *Cell* 1994;76:17–27.
31. DeGrendele HC, Estess P, Siegelman MH. Requirement for CD44 in activated T cell extravasation into an inflammatory site. *Science* 1997;278:672–5.
32. Caux C, Vanbervliet B, Massacrier C, Azuma M, Okumura K, Lanier LL, et al. B70/B7–2 is identical to CD86 and is the major functional ligand for CD28 expressed on human dendritic cells. *J Exp Med* 1994;180:1841–7.
33. Banchereau J, Steinman RM. Dendritic cells and the control of immunity. *Nature* 1998;392:245–52.
34. Gunzer M, Grabbe S. Dendritic cells in cancer immunotherapy. *Crit Rev Immunol* 2001;21:133–45.
35. Gong J, Chen D, Kashiwaba M, Li Y, Chen L, Takeuchi H, et al. Reversal of tolerance to human MUC1 antigen in MUC1 transgenic mice immunized with fusions of dendritic and carcinoma cells. *Proc Natl Acad Sci U S A* 1998;95:6279–83.
36. Gong J, Nikrui N, Chen D, Koido S, Wu Z, Tanaka Y, et al. Fusions of human ovarian carcinoma cells with autologous or allogeneic dendritic cells induce antitumor immunity. *J Immunol* 2000;165:1705–11.
37. Koido S, Hara E, Torii A, Homma S, Toyama Y, Kawahara H, et al. Induction of antigen-specific CD4- and CD8-mediated T-cell responses by fusions of autologous dendritic cells and metastatic colorectal cancer cells. *Int J Cancer* 2005;117:587–95.
38. Koido S, Ohana M, Liu C, Nikrui N, Durfee J, Lerner A, et al. Dendritic cells fused with human cancer cells: morphology, antigen expression, and T cell stimulation. *Clin Immunol* 2004;113:261–9.
39. Moser M, Murphy KM. Dendritic cell regulation of TH1-TH2 development. *Nat Immunol* 2000;1:199–205.
40. Perez O, Bracho G, Lastre M, Mora N, del Campo J, Gil D, et al. Novel adjuvant based on a proteoliposome-derived cochleate structure containing native lipopolysaccharide as a pathogen-associated molecular pattern. *Immunol Cell Biol* 2004;82:603–10.
41. Liu YJ. Dendritic cell subsets and lineages, and their functions in innate and adaptive immunity. *Cell* 2001;106:259–62.
42. Willmann K, Legler DF, Loetscher M, Roos RS, Delgado MB, Clark-Lewis I, et al. The chemokine SLC is expressed in T cell areas of lymph nodes and mucosal lymphoid tissues and attracts activated T cells via CCR7. *Eur J Immunol* 1998;28:2025–34.
43. Visintin A, Mazzoni A, Spitzer JH, Wylie DH, Dower SK, Segal DM. Regulation of Toll-like receptors in human monocytes and dendritic cells. *J Immunol* 2001;166:249–55.
44. Apetoh L, Ghiringhelli F, Tesniere A, Obeid M, Ortiz C, Criollo A, et al. Toll-like receptor 4-dependent contribution of the immune system to anticancer chemotherapy and radiotherapy. *Nat Med* 2007;13:1050–9.
45. Iwasaki A, Medzhitov R. Toll-like receptor control of the adaptive immune responses. *Nat Immunol* 2004;5:987–95.
46. Przetak M, Chow J, Cheng H, Rose J, Hawkins LD, Ishizaka ST. Novel synthetic LPS receptor agonists boost systemic and mucosal antibody responses in mice. *Vaccine* 2003;21:961–70.
47. Means TK, Jones BW, Schromm AB, Shurtleff BA, Smith JA, Keane J, et al. Differential effects of a Toll-like receptor antagonist on Mycobacterium tuberculosis-induced macrophage responses. *J Immunol* 2001;166:4074–82.
48. Bansal K, Elluru SR, Narayana Y, Chaturvedi R, Patil SA, Kaveri SV, et al. PE_PGRS antigens of mycobacterium tuberculosis induce maturation and activation of human dendritic cells. *J Immunol* 2010;184:3495–504.
49. Pecora ND, Gehring AJ, Canaday DH, Boom WH, Harding CV. Mycobacterium tuberculosis LprA is a lipoprotein agonist of TLR2 that regulates innate immunity and APC function. *J Immunol* 2006;177:422–9.

Cancer Research

The Journal of Cancer Research (1916–1930) | The American Journal of Cancer (1931–1940)

Enhanced Efficacy of Therapeutic Cancer Vaccines Produced by Co-Treatment with *Mycobacterium tuberculosis* Heparin-Binding Hemagglutinin, a Novel TLR4 Agonist

In Duk Jung, Soo Kyung Jeong, Chang-Min Lee, et al.

Cancer Res 2011;71:2858-2870. Published OnlineFirst March 2, 2011.

Updated version	Access the most recent version of this article at: doi: 10.1158/0008-5472.CAN-10-3487
Supplementary Material	Access the most recent supplemental material at: http://cancerres.aacrjournals.org/content/suppl/2011/03/02/0008-5472.CAN-10-3487.DC1

Cited articles	This article cites 48 articles, 20 of which you can access for free at: http://cancerres.aacrjournals.org/content/71/8/2858.full#ref-list-1
Citing articles	This article has been cited by 2 HighWire-hosted articles. Access the articles at: http://cancerres.aacrjournals.org/content/71/8/2858.full#related-urls

E-mail alerts	Sign up to receive free email-alerts related to this article or journal.
Reprints and Subscriptions	To order reprints of this article or to subscribe to the journal, contact the AACR Publications Department at pubs@aacr.org .
Permissions	To request permission to re-use all or part of this article, use this link http://cancerres.aacrjournals.org/content/71/8/2858 . Click on "Request Permissions" which will take you to the Copyright Clearance Center's (CCC) Rightslink site.